JOURNAL OF MATERIALS SCIENCE 29 (1994) 548–553

Effect of particles on interlaminar crack growth in cross-plied carbon-fibre/epoxy laminates

V. K. SRIVASTAVA*, B. HARRIS
School of Materials Science, University of Bath, Bath, BA2 7AY, UK

This paper discusses the effect of particulate additions on the mode-I and mode-II interlaminar fracture toughness of a cross-plied, carbon-fibre-reinforced, epoxy-resin laminate. Particles of graphite, silicon carbide and polyethylene were mixed with the epoxy resin prior to laminating with woven carbon-fibre cloth. Tests have been performed on double cantilever beam (DCB) and end-notched-flexure (ENF) specimens to obtain the critical-strain energy-release rates, G_{IC} and G_{IIC}, for the laminates with and without particulate additions. The dependences of the values of G_{IC} and G_{IIC} on the crack length are also considered. The results indicate that the interlaminar-fracture-toughness (mode-I and mode-II) values of the CFRP laminate increase with increases in the particle content up to about 3%, and thereafter they decrease with further increases in the particle content. This was thought to be due to an increase in multiple-crack formation in the middle region of the cracked-plate samples. Furthermore, mode-I tests indicate that the propagation values of G_{IC} are dependent on the crack length.

1. Introduction

Polymer composites are increasingly capturing the attention of materials scientists. In the aerospace industry, the availability of new composites which are stronger and tougher than conventional materials would be an asset, and efforts are being made to develop such materials. In the development of fibre composites, most attention has been concentrated on the behaviour of the material under the action of in-plane stresses. This behaviour is dominated by the properties of the fibres, and in carbon-fibre-reinforced plastics (CFRPs) the properties of the matrices tend to be regarded as being of relatively minor importance. In many practical uses of CFRPs, however, situations can occur in which dangerously high levels of stress may arise in the matrix resulting in crack propagation parallel to the fibres or at the fibre/matrix interface. The resistance of the composite to crack propagation parallel to the fibres is therefore of considerable importance. Since the initial growth of a crack in a direction parallel to the fibres is controlled by the toughness of the matrix, the use of tougher resins would be expected to lead to improvements in the matrix-dominated properties controlled by this failure mode [1–7]. Work on particle-filled fibre composites indicates that the fracture toughness was improved marginally, but significantly, while the fibre-dominated properties remained almost unchanged [6]. Studies on SiC-filled glass/phenolic composites have revealed increases in the compression, flexure, impact and interlaminar shear strengths with increasing additions of SiC after an initial reduction, whereas alumina-filled glass/epoxies showed an increase in interlaminar shear strength and a decrease in translaminar shear strength with increasing additions of alumina [6–7]. These results showed that crack propagation in the particle-filled-fibre composite is complex, with both crack-tip blunting and crack pinning taking place simultaneously. This suggests that both crack-tip blunting (by plastic yielding of the matrix) and crack pinning may be important as toughening mechanisms.

In this paper we present the results of an experimental program to study the effect of additions of particulate SiC, graphite and polyethylene on the mode-I and mode-II interlaminar fracture toughnesses of a carbon-fibre/epoxy composite. A comparison is made of the different methods of calculating the mode-I toughness from tests on double cantilever beam (DCB) samples. The variation of the mode-I toughness with crack length is also considered.

2. Basic analysis

A demand for the use of high-performance composites has generated extensive research concerned with improving the delamination or interlaminar-fracture properties of composites because the initiation and growth of a delamination may result in progressive stiffness degradation and may lead eventually to the failure of a composite structure. A delamination may initiate and grow at a free edge or at a stress raiser in a laminate under tensile or compressive loading applied quasi-statically or cyclically. It has been found that delamination resistance is increased by the use of matrices with higher toughnesses than those normally

* Also: Department of Mechanical Engineering, Institute of Technology, Banaras Hindu University, Varanasi 221 005, India

used. Several test methods have been developed for the evaluation of delamination behaviour. The most commonly used specimens at present are DCB specimens for mode-I and end-notch-flexure (ENF) specimens for mode-II.

2.1. Mode-I testing

The interlaminar fracture toughness, G_{IC}, can be determined from the DCB test by using data-reduction methods which give the strain-energy-release rate during both the crack initiation and propagation phases [8].

2.1.1. The compliance method

The compliance method is based on the assumption of beam-like behaviour of the delaminated half-sections of the specimen. The compliance, C, is assumed to be described by the beam-theory relationship

$$C = A_1 a^3 \tag{1}$$

where A_1 is an experimentally determined parameter which is geometry and material dependent, and a is the crack length. The strain-energy-release rate, G, is obtained from the formula

$$G = \frac{P^2}{2w}\frac{dC}{da} \tag{2}$$

where P is the applied load and w is the specimen width.
Differentiation of Equation 1 and substitution into Equation 2 yields

$$G = \frac{3A_1 P^2 a^2}{2w} \tag{3}$$

The critical condition occurs when crack growth is initiated at $P = P_c$ and $G = G_{IC}$. At the onset of crack growth, Equation 3 therefore yields

$$G_{IC} = \frac{3A_1 P_c^2 a^2}{2w} \tag{4}$$

2.1.2. The area method

The area method is a more direct method of establishing the fracture toughness. It is based on determination of the area, ΔA, enclosed within the loading and unloading load/displacement curves in a DCB test, and on determination of the increment, Δa, of new crack length [9]

$$G_{IC} = \frac{\Delta A}{w\Delta a} = \frac{P_1\delta_2 - P_1\delta_1}{2w\Delta a} \tag{5}$$

where P_1, P_2 and δ_1, δ_2 are the loads and displacements corresponding to the crack extension from a to $a + \Delta a$.

2.2. Mode-II Testing

The ENF test provides a method for determining the composite interlaminar fracture toughness in a forward-shear mode. The test specimen is essentially a three-point flexure specimen with an embedded through-width delamination at the laminate mid-plane where the interlaminar shear stress is greatest. The validity of the ENF test for inducing pure mode-II conditions at the mid-plane of woven-glass-fibre/epoxy specimens has been established and the effect of friction between the crack faces has been shown to be less than 4% [10].

An equation similar to Equation 2 can be written for the mode-II loading condition

$$G_{IIC} = \frac{P_c^2}{2w}\frac{dC}{da} \tag{6}$$

The relationship between the compliance, C, and the delamination length, a, is

$$C = (2L^3 + 3a^3)(8E_1wh^3) + \frac{1.2L + 0.9a}{4whG_{13}} \tag{7}$$

where L is the half-span and E_1 and G_{13} are the flexural and interlaminar shear moduli, respectively. The first and second terms in Equation 7 are due to the bending and interlaminar-shear components of deformation. Substitution of Equation 7 into Equation 6 yields

$$G_{IIC} = \frac{(9a^2P_c^2)}{(16E_1w^2h^3)[1 + 0.2(E_1/G_{13})(h/a)^2]} \tag{8}$$

In order to obtain an approximate estimate of the contribution of the interlaminar shear stress to G_{IIC}, the interlaminar shear modulus, G_{13}, is assumed to be the same as the in-plane shear modulus, G_{12}. Since the contribution of the interlaminar shear stresses to G_{IIC} is only marginal for isotropic-material systems, the second term in Equation 8 can be neglected. The simplified expression for the mode-II fracture toughness is therefore:

$$G_{IIC} = \frac{9a^2P_c\delta_c}{2w(2L^3 + 3a^3)} \tag{9}$$

3. Experimental procedures

The reinforcing material used was a balanced-weave carbon-fibre fabric (A0086 low modulus) supplied by Fothergill Engineered Fabrics Ltd., Lancashire, UK. The epoxy resin used was Araldite LY-5052 with a HY-5052 hardener. Graphite, silicon carbide and polyethylene were used as filler materials and the relevant characteristics of these materials are shown in Table I.

Laminates 2.2 mm thick (eight-ply) were prepared by the hand lay-up method at room temperature. Additions of the particulate materials, ranging from 0.5 to 7% by weight of the resin, were added to the epoxy resin before it was applied to the carbon-fibre cloth, care was taken to avoid agglomeration of the particles. In the following discussion, these materials will be referred to, for convenience, as G-CFRP (graphite-filled), S-CFRP (SiC-filled) and P-CFRP (polyethylene-filled). Teflon film (0.5 mm thick) was also inserted on the mid-plane at one edge of the laminate to provide a starter notch. The laminates

TABLE I Characteristics of the filler materials

Material	Particle size (μm)	Modulus (GPa)	Density ($kg\,m^{-3}$)	Tough/brittle response
SiC	5	450	3220	Very hard/brittle
Graphite	5	2.57	2250	Hard/brittle
Polyethylene	65	0.150	920	Soft/tough

were post-cured at 90 °C for 12 h, following the manufacturer's recommendations. The final fibre-volume fraction of all laminates was about 0.45.

The specimens used for the mode-I and mode-II tests were DCB and ENF configurations, respectively. The DCB specimens were 100 mm long, 20 mm wide and 2.2 mm thick. The starter notch length was 32 mm. Steel-hinge end tabs were glued onto the surfaces of the beam at the notch for application of the load to the specimen during testing. The sides of the specimen were painted white in order to permit visual crack-tip location.

The mode-II test was performed by three-point bending of the ENF-type specimens 64 mm long (the distance between the first and third pins) and 20 mm wide. The thickness was again 2.2 mm, and the pre-crack length was 16 mm.

The DCB and ENF tests were performed in an Instron 1195 test machine model at a cross-head speed of 5 mm min^{-1}. Once the crack in a DCB specimen (Fig. 1) had propagated a few millimetres, the increment of the crack length was measured. In order to avoid the resin-rich area in front of the starter notch, the crack after the first mode-I loading/unloading cycle, which was about 2 mm in length from the starter foil, was considered as the initial crack. Load/displacement curves for the DCB and ENF specimens were recorded by an *xy*-recorder for the determination of mode-I and mode-II toughnesses. All results reported were mean values from four separate samples.

Finally, the fractured surfaces of the DCB and ENF samples were examined by optical and scanning electron microscopy (SEM, Jeol T330).

4. Results and discussion

4.1. Effect of particles on mode-I toughness

From the loading and unloading curves of DCB samples of the plain CFRP and the filled composites, the relationship of the compliance, C, to the crack length, a, was obtained. To check the power-law dependence of the compliance on the crack length, the data were plotted as $C^{1/3}$ versus the crack length, a, as shown in Fig. 2. The results show that for all composites the compliance increased with increasing crack length in the manner given by Equation 1. This relationship is vital for the determination of the mode-I-strain-energy-release rate, G_{IC}.

The critical-strain energy-release rate (or interlaminar fracture toughness) was determined by both the compliance and the area methods and the results are shown in Figs 3 and 4. The values of G_{IC} obtained from the area method are higher than those from the compliance method by a factor of up to 2. The main reason for this is that the area method includes energy contributions other than those associated with the main interlaminar crack growth [11]. Each data point represents the average value of G_{IC} from four separate samples, and the error bars are standard deviations (SD). We acknowledge that the validity of an SD value determined from four results is suspect, but each of the four values contributing to each data point was in fact already the average of at least four separate determinations for separate increments of crack growth within a single test. In every case, the G_{IC}-values associated with the initial crack-growth increment were different from those of the subsequent G_{IC} growth values. Figs 3 and 4 show that the interlaminar fracture toughness of the CFRP laminate at first increased with increasing particle content up to a maximum at

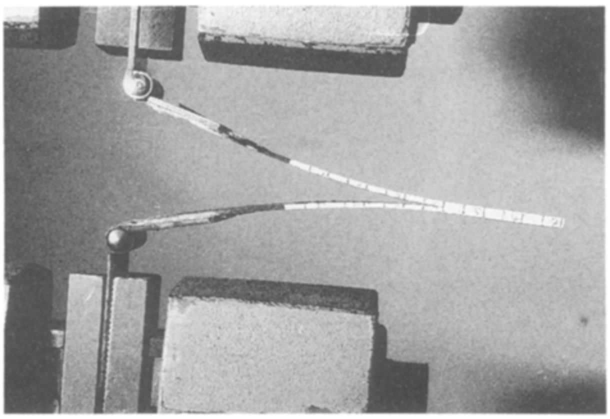

Figure 1 A photograph showing the propagation of a crack in a DCB test.

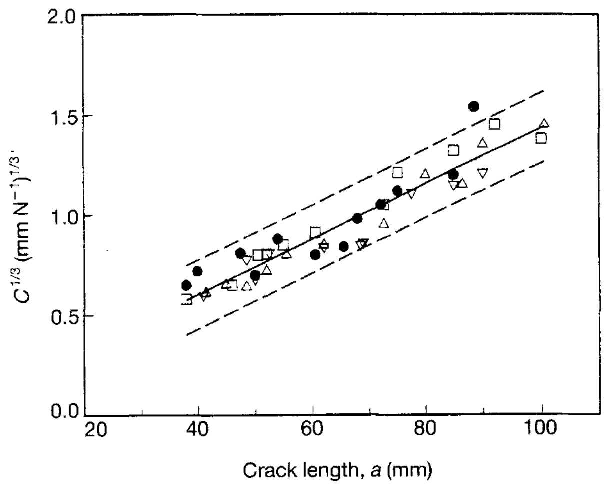

Figure 2 Relationship between the compliance and the crack length for filled and unfilled CFRP laminates (DCB experiments): (●) unfilled CFRP, (□) graphite filled, (△) Sic filled, (▽) polyethylene filled, and (- - -) 95% confidence limits. $c^{1/3} = 0.05 + 0.14a$; $r = 0.95$ (42 d of f).

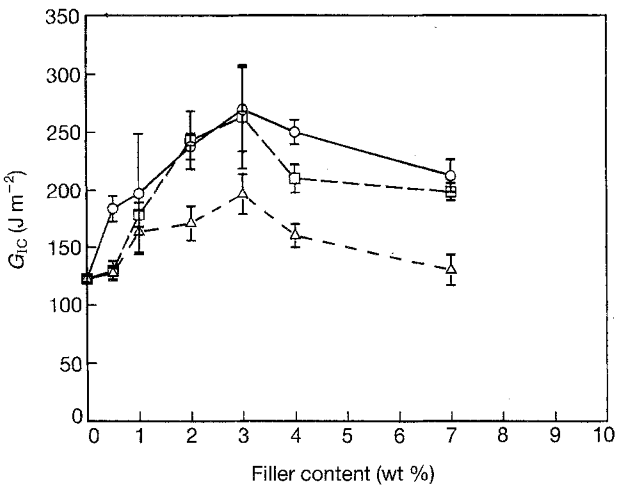

Figure 3 The effect of the filler content on the interlaminar fracture toughness, G_{IC}, (measured by the area method) for delamination growth in CFRP laminates: (○) graphite powder, (□) SiC powder, and (△) polyethylene powder.

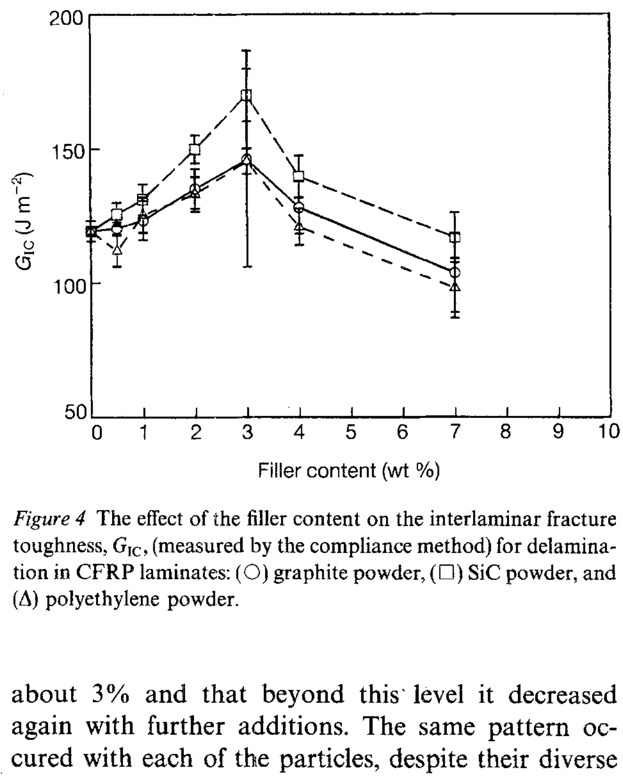

Figure 4 The effect of the filler content on the interlaminar fracture toughness, G_{IC}, (measured by the compliance method) for delamination in CFRP laminates: (○) graphite powder, (□) SiC powder, and (Δ) polyethylene powder.

about 3% and that beyond this level it decreased again with further additions. The same pattern occured with each of the particles, despite their diverse physical characteristics. These results are in agreement with the observation of Bradley and Cohen [12]. The graphite and silicon-carbide additions produce greater increases in the interlaminar fracture toughness than polyethylene, perhaps because the polyethylene particles are much larger and less effective than the particles of graphite and silicon carbide. The increases in fracture-toughness values are associated with an increase in the complexity of the crack-growth process. The primary crack makes detours around the obstacles which results in the initiation of secondary cracks as can be seen from Fig. 5a. From photographs of fractures there are no observed contributions from either particle bridging or plastic drawing of the polyethylene particles. This increased crack-surface area is thought to be one of the reasons for the observed increase in toughness of composite laminate [3].

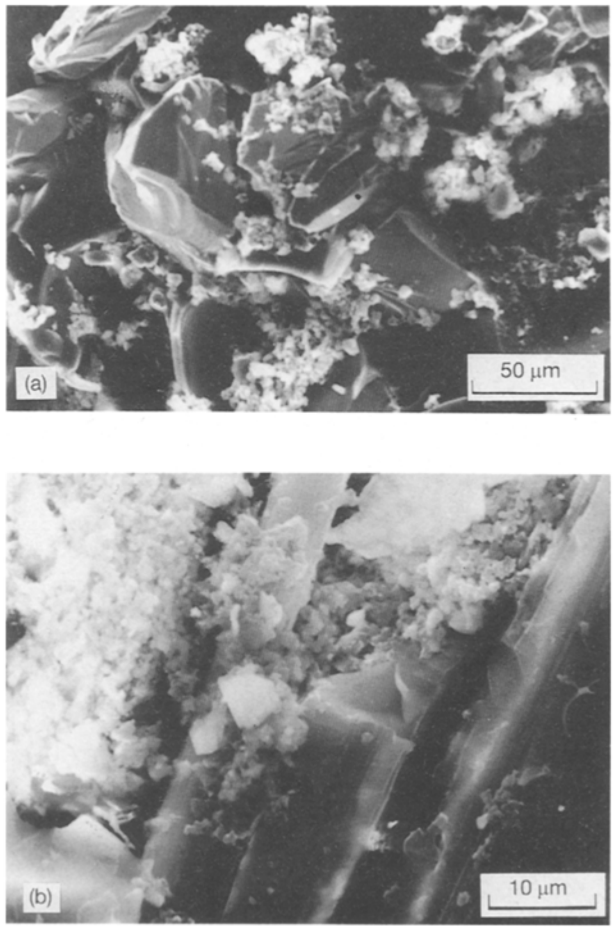

Figure 5 SEM fractographs showing: (a) crack detour around the particles, and (b) particles settled around the fibre.

4.2. Effect of crack length on the mode-I toughness

The G_{IC} values obtained from the compliance method with the corrected value, $a + \Delta a$, are shown in Fig. 6. These results show the clear effect of the crack length on the crack-propagation value of G_{IC}. The kind of rising R-curve shown in Fig. 6 is a commonly observed feature of tests of this type [4–5] and the implied increase in crack-growth resistance with increasing crack length is attributed to the growth of a tied zone of nested fibres bridging the crack faces. It should be pointed out that the specimen-to-specimen scatter shown in Fig. 6 is thought to be due to splitting in the vicinity of the crack tip. The initial value was calculated from the load at which initial-crack propagation from the insert occurs. After an increment of crack growth of about 4 mm, the specimens were unloaded and then re-loaded to obtain a second G_{IC}-value corresponding to another 4 mm increment of crack growth ahead of the insert. This method is a means of avoiding problems arising from the fibre disturbance and the resin-rich region usually associated with the presence of the insert [3]. It is clear that a CFRP laminate with about 3% particle filler gave higher fracture-toughness values with increases of crack length because of the good resin/particle interface. Small voids of different sizes in this DCB failed sample are seen in Fig. 7. This shows that the

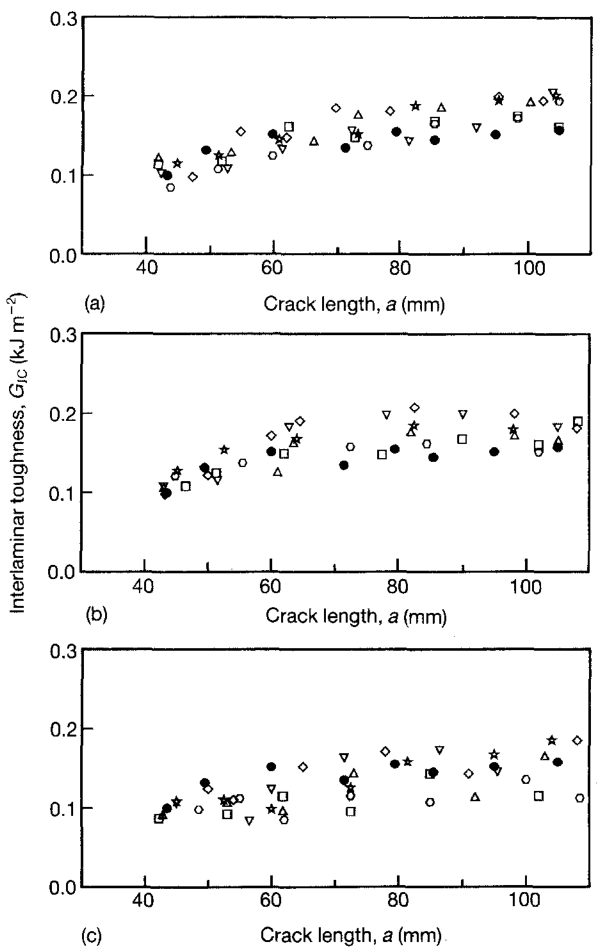

Figure 6 Variation of measured G_{IC} values with crack length for filled and unfilled CFRP laminates. The filled symbols show the *R*-curve behaviour of the unfilled composite. (a) Graphite filler, (b) SiC filler, and (c) Polyethylene filler: (□) 0.5%, (◇) 3%, (Δ) 1%, ★ 4%, (∇) 2% and (⬡) 7% filler content.

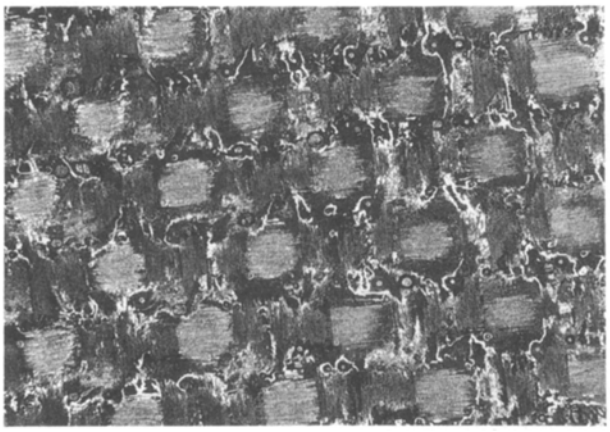

Figure 7 Optical micrograph showing a crack and a void near a resin-rich area.

crack growth occurs principally along the resin/fibre interface.

4.3. Effect of particles on the mode-II toughness

Fig. 8 indicates that the mode-II toughness, G_{IIC}, also increases with additions of graphite, silicon carbide and polyethylene particles, showing the same maximum, in the region of 3% addition, for all three types of particle, as that observed for the G_{IC}-values. Graphite and silicon-carbide additions again give higher G_{IIC}-values than the polyethylene additions, perhaps again because of their smaller particle size and the better adhesion between the inorganic fillers and the resin. These results suggest that the particles may be able to initiate debonding between the fibre and the matrix as can be identified from Fig. 5b, which increases the debonding energy and the toughness of the matrix material [8].

The two values of G_{IIC} reported in Fig. 8 give upper and lower bounds for G_{IIC} at initiation. In Fig. 8a it is assumed that the point of deviation from linearity indicates crack initiation. This may or may not be the case since initiation is observed by eye on the edge of the specimen after this point but before the maximum load. However, the crack front observed on the fracture surface is usually curved, with propagation at the specimen centre up to 4 mm longer than on the edges. The non-linearity may therefore be a result of initiation at the specimen centre, or because of non-linear elastic behaviour [13]. The value calculated at the point of non-linearity would then be a rather conservative upper-bound value; the inclusion of a calculated effective crack length is an assumption that the damage zone develops up to the maximum load, at which point macroscopic initiation takes place.

4.4. Comparison of mode-I and mode-II behaviour

The interesting feature of these results is that the mode-II interlaminar fracture toughness is a factor of about 10 higher than the mode-I toughness. In the ENF test, mode-II crack propagation causes relative sliding of the crack surfaces. Friction between the

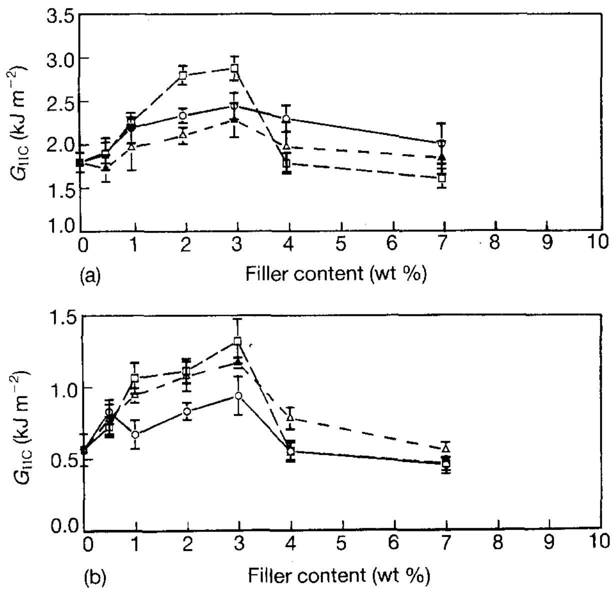

Figure 8 The effect of the filler content on the interlaminar fracture toughness, G_{IIC}, for delamination growth in CFRP laminates with the following fillers: (○) graphite powder, (□) SiC powder, and (Δ) polyethylene powder. (a) Maximum load, and (b) proportional limit.

crack surfaces may oppose the sliding and consequently increase the G_{IIC}-values because the sliding of crack surfaces is arrested by the particles. Mode-I and mode-II values are lower for polyethylene additions than for SiC and graphite additions. This indicates that the polyethylene filler is not very effective in reducing the friction due to the larger particles. However, the SiC filler has a tendency to settle on the fibre/matrix interface which gives higher mode-I and mode-II toughness values than the other fillers. Bradley and Cohen [12] observed similar behaviour in their work, and they attributed the difference to the unique nature of the fracture process in the mode-II test; namely, the formation of sigmoidally shaped microcracks for a considerable distance ahead of the crack tip, causing significant load redistribution.

5. Conclusions

1. Mode-I and mode-II crack-propagation values of G_{IC} and G_{IIC} increase with increasing weight percentages of filler. This can be improved by a factor of two to three by the addition of graphite, silicon carbide and polyethylene filler materials.

2. The area method of data reduction is valid provided the damage is dominated by interlaminar crack propagation during the mode-I test. The G_{IC} values show an increase in interlaminar fracture toughness with crack length.

3. The mode-II-interlaminar-fracture toughness values are 10 times higher than the mode-I values because of the different operative fracture mechanisms.

4. The mode-I and mode-II-interlaminar-fracture toughness values of G-CFRP and S-CFRP are higher than those of the P-CFRP laminate owing to the larger particle size of the polyethylene. But silicon-carbide-filled CFRP has higher interlaminar fracture toughnesses in mode-I and mode-II than the other laminates. This effect of SiC particles has been attributed to the decrease in void formation and to a tendency to settle at the carbon-fibre/resin interface.

Acknowledgements

This work was carried out at School of Materials Science, University of Bath, Bath, BA2 7AY, UK, with the financial support of the European Communities, Brussels, Belgium. One of us (V. K. Srivastava) was the recipient of a EC post-doctoral fellowship.

References

1. J. M SCOTT and D. C. PHILLIPS, *J. Mater. Sci.* **10** (1975) 551.
2. M. XANTHOS and R. T. WOODHAMS, in the Twenty-Ninth Annual Conference SPI, (1974).
3. S. FANG and D. D. L. CHUNG, *Composites* **21** (1990) 419.
4. V. BALAKRISHNA, KISHORE and D. S. CHANDRA, *J. Mater. Sci. Lett.* **11** (1992) 1154.
5. D. S. CHANDRA, G. S. AVADHANI and KISHORE, *J. Mater. Sci. Engng A* **136** (1991) 179.
6. H. M. CHENG, A. KITAHARA, K. KOBAYASHI and B. L. ZHOU, *J. Mater. Sci. Lett.* **10** (1991) 795.
7. H. M. CHENG, A KITAHARA, S. AKIYAMA, K. KOBAYASHI and B. L. ZHOU, *J. Mater. Sci.* **27** (1992) 3617.
8. D. J. WILKINS, J. R. EISENMANN, R. A. CHAMIN, W. S. MARGOLIS and R. A. BENSON, ASTM STP 775 edited by K.L. Reifsnider (American Society for Testing Materials, Philadelphia, 1982) 168.
9. J. W. GILLESPIE Jr, L. A. CARLSSON and A. J. SMILEY, *Comp. Sci. Tech.* **28** (1987) 1.
10. L. A. CARLSSON, J. W. GILLESPIE and R. B. PIPES, *J. Comp. Mater.* **20** (1986) 594.
11. J. M. WHITNEY, C. E. BROWNING and W. HOOGSTEDEN, *J. Rein. Past. Comp.* **1** (1987) 1.
12. W. L. BRADLEY and R. N. COHEN, ASTM STP 876 edited by W. S. Johnson (American Society for Testing and Materials, Philadelphia, 1985) 389.
13. P. DAVIES, C. MOULIN, H. H. KAUSCH and M. FISCHER, *Comp. Sci. Tech.* **39** (1990) 193.

Received 24 April
and accepted 9 July 1993